Cancer Chemother Pharmacol (2001) 47: 291–302
DOI 10.1007/s002800000242

ORIGINAL ARTICLE

**Merrill J. Egorin · Eleanor G. Zuhowski
D. Marc Rosen · Dorothy L. Sentz
Joseph M. Covey · Julie L. Eiseman**

Plasma pharmacokinetics and tissue distribution of 17-(allylamino)-17-demethoxygeldanamycin (NSC 330507) in CD2F1 mice1

Received: 9 June 2000 / Accepted: 6 November 2000 / Published online: 11 January 2001

Abstract *Purpose*: 17-(Allylamino)-17-demethoxygeldanamycin (17AAG) is a benzoquinone ansamycin compound agent that has entered clinical trials. Studies were performed in mice to: (1) define the plasma pharmacokinetics, tissue distribution, and urinary excretion of 17AAG after i.v. delivery; (2) to define the bioavailability of 17AAG after i.p. and oral delivery; and (3) to characterize the concentrations of 17AAG metabolites in plasma and tissue. *Materials and methods*: All studies were performed in female CD_2F_1 mice. Preliminary toxicity studies used 17AAG i.v. bolus doses of 20, 40 and 60 mg/kg. Pharmacokinetic studies used i.v. 17AAG doses of 60, 40, and 26.67 mg/kg and i.p. and oral doses of 40 mg/kg. The plasma concentration versus time data were analyzed by compartmental and noncompartmental methods. The concentrations of 17AAG were also determined in brain, heart, lung, liver, kidney, spleen, skeletal muscle, and fat. Urinary drug excretion was calculated until 24 h after treatment. *Results*: A 60 mg/kg dose of 17AAG, in its initial, microdispersed formulation, caused no changes in appearance, appetite, waste elimination, or survival of treated animals as compared to vehicle-treated controls. Bolus i.v. delivery of 60 mg/kg microdispersed 17AAG produced "peak" plasma 17AAG concentrations between 5.8 and 19.3 μg/ml in mice killed 5 min after injection. Sequential reduction of the 17AAG dose to 40 and 26.67 mg/kg resulted in "peak" plasma 17AAG concentrations between 8.9 and 19.0 μg/ml, and 4.8 and 6.1 μg/ml, respectively. Noncompartmental analysis of the plasma 17AAG concentration versus time data showed an increase in AUC from 402 to 625 and 1738 μg/ml·min when the 17AAG dose increased from 26.67 to 40 and 60 mg/kg, respectively. Across the range of doses studied, 17AAG total body clearance varied from 34 to 66 ml/min per kg. Compartmental modeling of the plasma 17AAG concentration versus time data showed that the data were fitted best by a two-compartment, open, linear model. In each study, substantial concentrations of a material, subsequently identified as 17-(amino)-17-demethoxygeldanamycin (17AG), were measured in plasma. A subsequent, lyophilized formulation of 17AAG proved excessively toxic when delivered i.v. at 60 mg/kg. A repeat i.v. study using a 40 mg/kg dose of this new formulation produced peak plasma 17AAG concentrations of 20.2–38.4 μg/ml, and a 17AAG AUC of 912 μg/ml·min, which was approximately 50% greater than the AUC produced by a 40 mg/kg dose of microdispersed 17AAG. The bioavailabilities of 17AAG after i.p. and oral delivery were 99% and 24%, respectively. Minimal amounts of 17AAG and 17AG were detected in the urine. After i.v. bolus delivery to mice, 17AAG distributed rapidly to all tissues, except the brain. Substantial concentrations of 17AG were measured in each tissue.

Supported by contract NO1-CM57199 and Grant 2P30 CA47904, awarded by the National Cancer Institute.

M. J. Egorin (✉) · E. G. Zuhowski · D. M. Rosen
D. L. Sentz · J. L. Eiseman
Division of Developmental Therapeutics,
University of Maryland Cancer Center, Baltimore,
MD 21201, USA

M. J. Egorin
Division of Hematology/Oncology,
Department of Medicine, University of Maryland School of Medicine, Baltimore, MD 21201, USA

J. M. Covey
Toxicology and Pharmacology Branch,
Developmental Therapeutics Program,
Division of Cancer Treatment and Diagnosis,
National Cancer Institute, Bethesda, MD 20892, USA

J. L. Eiseman
Department of Pathology,
University of Maryland School of Medicine,
Baltimore, MD 21201, USA

M. J. Egorin
Present address: University of Pittsburgh Cancer Institute,
E1040 Biomedical Sciences Tower, 200 Lothrop Street,
Pittsburgh, PA 15213, USA
E-mail: egorinmj@msx.upmc.edu
Tel.: +1-412-6249272; Fax: +1-412-6489856

Conclusions: 17AAG has excellent bioavailability when given i.p. but only modest bioavailability when given orally and is metabolized to 17AG and other metabolites when given i.v., i.p., or orally. 17AAG is widely distributed to tissues. These pharmacokinetic data generated have proven relevant to the design of recently initiated clinical trials of 17AAG and could be useful in their interpretation.

Key words Geldanamycin · Ansamycin · HSP90 · Pharmacokinetics

Introduction

Geldanamycin (Fig. 1), a benzoquinone ansamycin antibiotic related to herbimycin A, has potent antiproliferative activity [5, 22, 28, 33, 34, 39]. Furthermore, this antiproliferative activity correlates with the ability of geldanamycin to deplete $p185^{erbB2}$, mutant p53, and Raf-1 [5, 22, 28, 33, 34, 39]. Although the exact mechanisms by which geldanamycin depletes cells of these oncoproteins is still being characterized, it is thought to be mainly related to the ability of geldanamycin to bind specifically to the heat shock protein hsp90 and its homologue GRP94, and thereby destabilize the heteroprotein complexes they form with oncoproteins [5, 11, 18, 25, 26, 32, 35, 38, 43, 44].

As part of an effort to develop novel, potent, and selective inhibitors of $p185^{erbB2}$ that might also be useful antitumor agents, a number of geldanamycin derivatives have been synthesized and characterized biologically to varying degrees [33, 34]. One of these derivatives, 17-(allylamino)-17-demethoxygeldanamycin (17AAG, NSC 330507), has been selected for clinical development and has recently been introduced into phase I testing [3, 8, 12]. As part of the preclinical evaluation in preparation for clinical trials, we performed pharmacokinetic studies of 17AAG in mice. Our intention was to define the plasma pharmacokinetics, tissue distribution, and bioavailability of 17AAG, and, if possible, also study its metabolism [15].

Materials and methods

Reagents

Triethylamine and α-naphthoflavone were obtained from Sigma Chemical Co. (St. Louis, Mo.) and Aldrich Chemicals (Milwaukee, Wis.), respectively. 17-(Amino)-17-demethoxygeldanamycin (17AG, NSC 255109; Fig. 1) was obtained from the Developmental Therapeutics Program, National Cancer Institute (Bethesda, Md.). Ethyl acetate and acetonitrile (Baker analyzed grade) were obtained from J.T. Baker (Phillipsburg, N.J.).

Drug

17AAG was initially supplied by the National Cancer Institute as a microdispersed preparation in 4% egg phospholipid and 5% dextrose and was subsequently provided as a lyophilized preparation containing sucrose instead of dextrose. Both preparations were supplied in 10-ml clear glass serum vials. The microdispersed preparation contained 10 ml 17AAG at a concentration of 5 mg/ml. The lyophilized preparation contained either 2.5 or 10 mg per vial. Vials were stored in the dark and at 4–8°C until use. The lyophilized preparation was reconstituted by the addition of the appropriate volume of sterile pyrogen-free water.

Mice

Specific pathogen-free adult female CD_2F_1 mice (5–6 weeks of age) were obtained from the Animal Program administered by the Animal Genetics and Production Branch of the National Cancer Institute. Mice were allowed to acclimate to the University of Maryland Baltimore Animal Facility for at least 1 week before

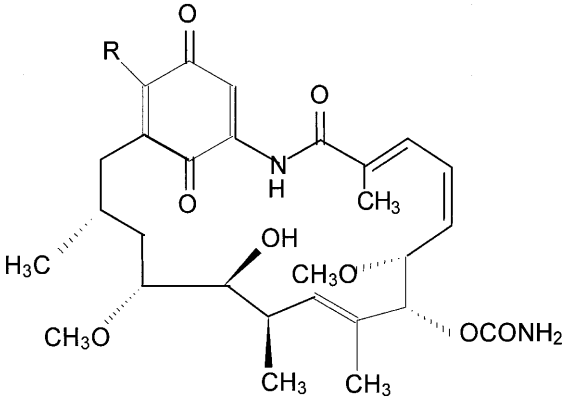

Fig. 1 Structures of geldanamycin, 17-(allylamino)-17-demethoxygeldanamycin and 17-(amino)-17-demethoxygeldanamycin

Compound	R	Molecular Weight
Geldanamycin	CH_30	560
17-(allylamino)-17-demethoxygeldanamycin	CH_2=CH-CH_2-NH	585
17-(amino)-17-demethoxygeldanamycin	NH_2	545

studies were initiated. To minimize exogenous infection, mice were maintained in microisolator cages in a separate room and handled in accordance with the Guide for the Care and Use of Laboratory Animals (National Research Council, 1996). Ventilation and air flow in the animal facility were set to 12 changes per hour. Room temperatures were regulated at 72 ± 2°F, and the rooms were kept on automatic 12-h light/dark cycles. Mice received Teklad LM-484 sterilizable mouse diet (Harlan Teklad Diets, Madison, Wis.) and water ad libitum except on the evening prior to dosing when all food was removed and withheld until 4 h after dosing. Sentinel mice (CD-1 mice in cages with bedding that contained 20% bedding removed from study mouse cages at cage change) were maintained in the animal room and assayed at monthly intervals for specific murine pathogens by murine antibody profile testing (Litton Bionetics, Charleston, S.C.). These mice remained free of specific pathogens throughout the study period, indicating that the study mice were free of specific pathogens.

Protein binding studies

In order to assess protein binding of 17AAG, solutions of 17AAG were prepared in mouse plasma, and aliquots were placed into Amicon Centrifree ultrafiltration devices (Amicon Company, Danvers, Mass.). After centrifugation of the ultrafiltration devices for 20 min at room temperature and 2000 *g*, the concentrations of 17AAG in the resulting protein-free ultrafiltrates and in the initial plasma solutions were determined with the HPLC method described below.

Range-finding study in mice

Groups of five female CD_2F_1 mice were dosed i.v. with 20, 40 or 60 mg/kg 17AAG or vehicle. Mice were observed for 14 days after dosing. Clinical observations were made twice daily. Body weights were measured twice weekly. All group data, including necropsy tissue weights, were compared by both parametric and nonparametric methods using Minitab (Minitab, State College, Pa.). If one-way analysis of variance was significant, pair-wise comparisons were made using Dunnett's *t*-test. Nonparametric analyses used the Kruskal-Wallace test followed by pair-wise comparisons using the Mann-Whitney test.

Pharmacokinetic studies

Dosing

Drug solutions were adjusted with vehicle such that each mouse at doses of 40 and 26.67 mg/kg received 0.01 ml/g fasted body weight. Mice dosed with 60 mg/kg received 0.012 ml/g fasted body weight. 17AAG i.v. doses were administered as boluses through a 27-gauge needle placed into a lateral tail vein. 17AAG i.p. doses were delivered with a 27-gauge needle placed into the left lower abdominal quadrant. 17AAG oral doses were delivered with a 1.5-in 22-gauge curved gavage needle. The accuracy of each dosing solution was confirmed with the HPLC method described below.

Sampling

In all studies, blood was sampled at 5, 10, 15, 30, 45, 60, 90, 120, 180, 240, 360, 420, 960, and 1440 min after dosing. In the studies in which the initial formulation of 17AAG was administered i.v. at 60 mg/kg and a later study in which it was delivered i.v. in a subsequent formulation at 40 mg/kg, brain, heart, lungs, liver, kidneys, spleen, fat and skeletal muscle were collected from each mouse at the same times noted for the blood samples. In each study, blood and, if relevant, tissues from mice killed 5 min after delivery of vehicle served as controls. Blood was collected by cardiac puncture into heparinized syringes, transferred to Eppendorf microcentrifuge tubes and stored on ice until centrifuged at 13,000 *g* for 5 min to obtain plasma. Tissues were rapidly dissected, placed on ice until weighed, and then snap-frozen in liquid nitrogen. Sets of animals to be sampled at 960 or 1440 min after dosing were gang-housed in metabolism cages, and urine was collected on ice until animals were killed for blood and, if necessary, tissue sampling. Plasma, tissues, urine and dosing solutions were stored at –70°C until analyzed.

Analysis of in vivo samples

Plasma, tissue, and urinary concentrations of 17AAG and metabolites were determined by HPLC, using a modification of a previously published method [15]. Plasma samples were extracted directly. Tissue samples were thawed and immediately homogenized using a Polytron (Brinkman Instruments, Westbury, N.Y.), in two to four parts (weight to volume) of phosphate-buffered saline (1.2 m*M* KH_2PO_4, 2.9 m*M* Na_2HPO_4, 154 m*M* NaCl, pH 7.4; Biofluids, Rockville, Md.).

Extraction procedure

To a 200-µl sample of plasma or tissue homogenate, 5 µl of 25 µg/ml α-naphthoflavone (internal standard) in acetonitrile was added and mixed. Each sample was extracted with 1 ml ethyl acetate by mixing for 10 min on a Vortex Genie 2 (Model G-560; Scientific Industries, Bohemia, N.Y.) set at 5. The samples were subsequently centrifuged at 12,000 *g* for 5 min, and the resulting organic layers were removed and transferred to 12 × 75 mm glass culture tubes. Each sample was extracted with an additional 1 ml ethyl acetate, vortexed, centrifuged, and the second organic layers were combined with the first. The organic layers were evaporated to dryness under a stream of nitrogen, and the dried residues were resuspended in 225 µl of the mobile phase described below. These samples were transferred to microcentrifuge tubes and centrifuged at 12,000 *g* for 5 min. The resulting supernatants were placed into glass microvial inserts, and 175 µl was injected by autosampler into the HPLC system.

HPLC

The HPLC system consisted of a Waters WISP 712B autosampler (Waters Associates, Milford, Mass.) and a Waters 501 pump fitted with a Waters Novapak C18 guard column and a Waters Novapak C18 column (5 µm, i.d. 3.9×150 mm). The isocratic mobile phase, consisting of acetonitrile/25 m*M* sodium phosphate, pH 3.00 (40:60 v/v) with 10 m*M* triethylamine, was pumped at 1 ml/min. Column eluent was monitored with a Waters 440 detector fitted with 313 nm filter and slit. Under these conditions, the retention time of 17AAG and internal standard were approximately 17 and 28 min, respectively, and the overall run time was 33 min. Standard curves, prepared in plasma or control tissue homogenates, were performed in duplicate. Plasma standard curves included 17AAG concentrations of 0.05, 0.1, 0.3, 1, 3, 10, and 15 µg/ml. Tissue standard curves also included 17AAG concentrations of 30, 100, 300, and 600 µg/ml. There were no endogenous materials in mouse plasma, any mouse tissue, or dosing vehicle that interfered with determination of 17AAG or internal standard.

Recovery of 17AAG from spiked samples containing 10 µg/ml was 100 ± 2.3% ($n = 3$). The lower limit of quantitation [36] in plasma and tissue homogenates was 0.1 µg/ml. The within-day ($n = 3$) coefficients of variation in plasma at a low mid-range concentration (0.3 µg/ml) and a high mid-range concentration (3 µg/ml) were 2.2–8.5% and 6.2–9.2%, respectively. The between-day coefficients of variation of these same concentrations were 10.5% and 11.3%, respectively. The standard curve of 17AAG in plasma was linear between 0.1 and 15 µg/ml. The standard curves of 17AAG in tissue homogenates were linear between 0.1 and 600 µg/ml. Plasma quality control samples,

prepared at 0.1 and 2.5 μg/ml and stored at –20°C, were included with each HPLC run. Samples containing concentrations above the upper limits of each standard curve were reassayed after dilution in the appropriate matrix to a degree calculated to produce concentrations within the linear range. Tissue concentrations of 17AAG and 17AG were expressed as micrograms per gram, based on the assumption that the weight of 1 ml of homogenate was 1 g.

Pharmacokinetic analysis

The time courses of the plasma concentrations of 17AAG were analyzed by both noncompartmental and compartmental methods. The area under the curve from zero to infinity (AUC) and the terminal half-life ($t_{1/2}$) were estimated by noncompartmental analysis using the LaGrange function [45] as implemented by the computer program LAGRAN [29]. Total body clearance (CL_{tb}) was calculated from the equation:

$$CL_{tb} = \text{dose}/\text{AUC}$$

and the steady-state volume of distribution (Vd_{ss}) was calculated from the equation:

$$Vd_{ss} = \text{dose} \times (\text{AUMC}/\text{AUC}^2)$$

where AUMC is the area under the moment curve from zero to infinity. Tissue AUCs were also calculated using the LaGrange function.

Individual concentrations of 17AAG detected in plasma versus time were fitted to compartmental models with the program ADAPT II [13] using maximum likelihood estimation. Two- and three-compartment open linear models were fitted to the data. Model discrimination was based on Akaike's information criterion (AIC) [4], calculated as:

$$AIC = 2p + n(\ln WSSR)$$

where p represents the number of parameters, *n* is the number of observations and WSSR is the weighted sum of squares residuals.

Results

Plasma protein binding

When a 10 μg/ml solution of 17AAG in 0.154 *M* NaCl was centrifuged in a Centrifree device, there was no measurable binding of 17AAG to the ultrafiltration membrane. When 0.5 and 5 μg/ml solutions of 17AAG in mouse plasma were processed in a similar manner, $7.2 \pm 2.6\%$ (mean ± SD) and $8.8 \pm 1.1\%$ of the 17AAG was ultrafilterable, indicating that $>90\%$ of the 17AAG was protein-bound.

Range-finding study

With the initial microdispersed 17AAG formulation, no changes were noted in appearance, appetite, waste elimination or body weight of treated animals when compared to untreated controls. Upon gross necropsy, the only notable findings were that the kidneys in all the drug-treated groups were pale, and a statistically significant, though slight, elevation in spleen weight was noted in the 20 mg/kg group (0.107 ± 0.011 g vs 0.089 ± 0.010 g in the control group, $P < 0.05$).

Pharmacokinetic studies

Because no untoward effects were noted in the range-finding study, the maximum dose used in the i.v. pharmacokinetic studies was 60 mg/kg. This maximum dose also reflected the solubility of 17AAG in the vehicle and the volume that could be delivered i.v. to mice.

Microdispersed formulation

Plasma pharmacokinetics. After an i.v. dose of 60 mg/kg, "peak" plasma 17AAG concentrations 5 min after injection were 5.8–19.3 μg/ml (Fig. 2A). Thereafter, plasma 17AAG concentrations declined in a manner best fitted by a two-compartment open linear model (Table 1) and after 960 min were below the lower limit of quantitation. When calculated with noncompartmental methods, the 17AAG AUC produced by a 60 mg/kg i.v. dose was 1738 μg/ml·min, corresponding to a CL_{tb} of 34 ml/min per kg (Table 2). Sequential dose reduction to 40 and 26.67 mg/kg resulted in the expected lower plasma 17AAG concentrations and AUCs (Fig. 2B, C; Table 2). Following i.v. doses of 40 and 26.67 mg/kg, "peak" plasma 17AAG concentrations of between 8.9 and 19.0 and 4.8 and 6.1 μg/ml were found, respectively. As with the 60 mg/kg i.v. dose, the 17AAG concentration versus time profiles resulting from the 40 and 26.67 mg/kg doses were best fitted by a two-compartment open linear model (Table 1). The 17AAG AUCs resulting from the 40 and 26.67 mg/kg i.v. doses were 625 and 402 μg/ml·min, respectively, corresponding to CL_{tb} values of 64 and 66 ml/min per kg, respectively (Table 2).

A consistent observation in each of these studies was the appearance in the plasma of a material that was not present in plasma of vehicle-treated control mice or in the dosing solution used in any study (Fig. 2A, B, C). This material was more polar than 17AAG, having a retention time of approximately 4 min in the HPLC chromatogram. Moreover, the time-course of this material in plasma was consistent with that of a metabolite, increasing during the first 30–45 min after 17AAG delivery and then decreasing progressively during the remainder of each study. As with the parent compound, there was relatively little inter-animal variability in the plasma concentrations of this material at each time studied. Because the identity of this metabolite (subsequently identified as 17AG) was not known at the time these studies were performed, authentic standard was not available for construction of appropriate standard curves. However, subsequent studies demonstrated that the standard curves for 17AAG and 17AG were nearly superimposable. This allowed noncompartmental calculation of the AUCs of 17AG (Tables 3 and 4).

Urinary excretion. There was minimal urinary excretion of 17AAG. During the 24 h after i.v. dosing of 60, 40, or 26.67 mg/kg, between 2.0% and 3.2% of the delivered dose could be accounted for in the urine. Roughly half

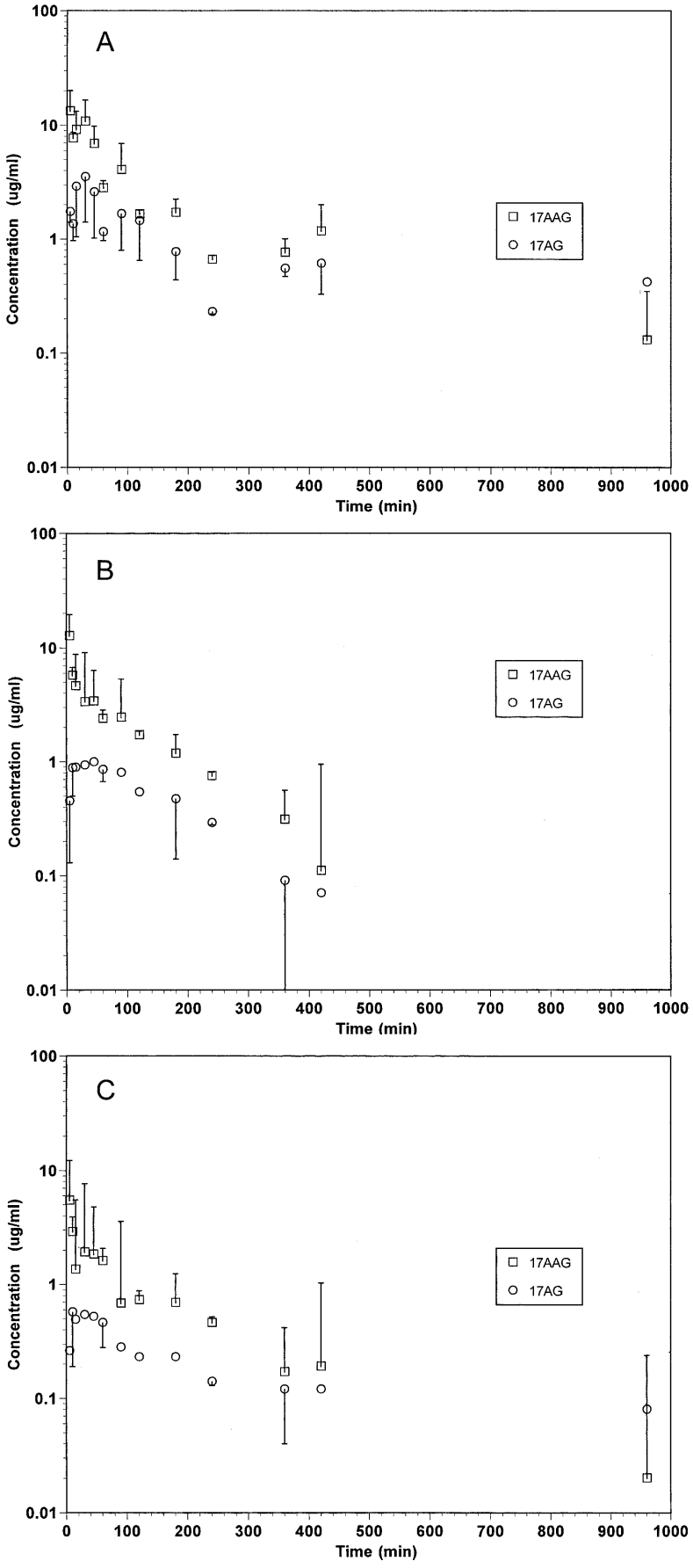

Fig. 2A–C Concentrations of 17AAG (□) and 17AG (○) detected in plasma of female CD_2F_1 mice given a microdispersed formulation of 17AAG i.v. at doses of (**A**) 60, (**B**) 40, or (**C**) 26.67 mg/kg. Symbols represent the means from three mice at each time-point, and error bars represent one SD

Table 1 Pharmacokinetic parameters resulting from fitting of compartmental models to plasma 17AAG concentration-versus-time data (V_c volume of the central compartment, k_e elimination constant, k_{cp} transfer constant between central and peripheral compartments, k_{pc} transfer constant between peripheral and central compartment, K_a absorption constant, $t_{1/2\alpha}$ alfa half-life, $t_{1/2\beta}$ beta half-life, CL_{tb} total body clearance, V_{dss} steady-state volume of distribution; *n.a.* not applicable)

Dose (mg/kg)	Formulation	Route	V_c (ml/kg)	k_e (min^{-1})	k_{cp} (min^{-1})	k_{pc} (min^{-1})	K_a (min^{-1})	$t_{1/2\alpha}$ (min)	$t_{1/2\beta}$ (min)	CL_{tb} ($ml \cdot min^{-1} \cdot kg$)	V_{dss} (ml/kg)
60	Microdispersed	i.v.	4536	0.010	0.009	0.005	n.a.	32	309	44	12,800
40	Microdispersed	i.v.	610	0.089	0.261	0.034	n.a.	2	87	54	5,354
26.67	Microdispersed	i.v.	1761	0.042	0.194	0.047	n.a.	2	96	74	8,970
40	Lyophilized	i.v.	769	0.048	0.081	0.030	n.a.	5	73	37	2,863
40	Lyophilized	i.p.	1445	0.029	n.a.	n.a.	0.030	23	n.a.	43[a]	n.a.
40	Lyophilized	oral	3744	0.056	0.045	0.008	0.041	7	n.a.	208[a]	23,760

[a]Apparent clearance

Table 2 Non-compartmental pharmacokinetic analyses of 17AAG plasma concentration-versus-time curves ($AUC_{0\text{-}inf}$ area under the curve from time zero to infinity, $t_{1/2}$ terminal half-life, V_{dss} steady-state volume of distribution, CL_{tb} total body clearance, *n.a.* not applicable)

Dose (mg/kg)	Formulation	Route	$AUC_{0\text{-}inf}$ ($\mu g \cdot ml^{-1} \cdot min$)	$t_{1/2}$ (min)	V_{dss} (ml/kg)	CL_{tb} ($ml \cdot min^{-1} \cdot kg$)	Bioavailability (%)
60	Microdispersed	i.v.	1738	239	10,200	34	n.a.
40	Microdispersed	i.v.	625	80	7,370	64	n.a.
26.67	Microdispersed	i.v.	402	159	14,300	66	n.a.
40	Lyophilized	i.v.	912	53	31,500	44	n.a.
40	Lyophilized	i.p.	900	23	32,600	44[a]	99
40	Lyophilized	oral	222	71	31,900	180[a]	24

[a]Apparent clearance

Table 3 AUCs (μg/ml·min) of 17AG in plasma and tissues of mice injected i.v. with a 60 mg/kg dose of microdispersed 17AAG

Plasma	Brain	Heart	Lung	Liver	Kidney	Spleen	Skeletal muscle
1362	66	1285	4241	8721	2215	1474	0

Table 4 AUCs (μg/ml·min) of 17AG in plasma and tissues of mice injected i.v. with a 40 mg/kg dose of lyophilized 17AAG

Plasma	Brain	Heart	Lung	Liver	Kidney	Spleen	Skeletal muscle
119	74	683	1141	4437	1942	1270	342

of this was present as parent compound and half as 17AG. Several other 17AAG metabolites were present in the urine [15], but their quantitative contributions to the urinary excretion of 17AAG was negligible.

Tissue distribution. Analyses of tissue concentrations of 17AAG allowed description of the widespread distribution of the drug, the relative inability of 17AAG to cross the blood-brain barrier, and the relative exposures of tissues as opposed to plasma. After i.v. delivery of a 60 mg/kg dose, 17AAG was widely distributed to tissues (Table 5). The highest tissue concentrations of 17AAG were observed in lungs, with progressively lower concentrations being present in liver, spleen, heart, kidney, brain, and skeletal muscle. In fact, the 5-min concentrations of 17AAG in lung, liver, spleen, heart and kidney exceeded the 5-min plasma 17AAG concentration by approximately 82-, 25-, 8-, 5-, and 4-fold, respectively. Although 17AAG concentrations in all tissues declined with time, 17AAG was detected in all tissues for at least 8 h after drug delivery and persisted in lung, spleen and liver for the 24-h duration of the study (Table 5). When expressed as AUC, the exposure of most tissues to 17AAG was substantially greater than that of plasma (Table 6). As with plasma, each organ contained substantial concentrations of the metabolite later identified as 17AG (Table 7).

Lyophilized formulation

After completion of the three i.v. pharmacokinetic studies described above, an effort was made to define the bioavailability of 17AAG after i.p. and oral delivery. However, before these studies could be undertaken, the formulation of 17AAG was revised from a microdispersed to a lyophilized preparation. As a result, a fourth i.v. pharmacokinetic study was undertaken so that the results of subsequent i.p. and oral studies could be compared with those of an i.v. study that used the same formulation. Although it was intended that these i.v., i.p., and oral studies would use a dose of 60 mg/kg, the new formulation of 17AAG proved lethal to five of the first eight mice given 60 mg/kg i.v. Therefore, in the

Table 5 Concentrations of 17AAG in plasma (μg/ml) and tissues (μg/g) of mice injected i.v. with a 60 mg/kg dose of microdispersed 17AAG

Time (min)	Plasma	Brain	Heart	Lung	Liver	Kidney	Spleen	Skeletal muscle
5	13.25[a]	4.03	69.89	1093.18	332.06	50.86	107.71	2.23
10	7.67	3.52	42.09	781.52	309.14	29.22	89.03	2.30
15	9.10	2.90	42.96	712.37	291.50	25.51	203.66	1.53
30	10.78	2.27	27.2	739.24	212.34	17.15	89.41	1.60
45	6.86	2.56	32.62	454.85	236.29	12.66	87.55	1.70
60	2.79	2.41	9.64	511.57	185.28	10.85	108.82	1.26
90	4.04	3.28	21.03	546.57	175.82	7.01	60.07	1.31
120	1.65	1.48	21.18	521.61	519.12	3.77	65.43	1.08
180	1.70	1.66	18.92	482.72	158.65	7.40	39.22	0.84
240	0.66	1.47	12.46	433.20	116.16	1.77	42.55	0.82
360	0.76	0.72	5.72	332.90	47.8	0.0	33.87	0.24
420	1.17	0.60	7.12	244.14	25.92	0.0	21.18	0.25
960	0.13	0.13	0.88	44.80	1.95	0.0	3.38	0.0
1440	0.0	0.09	0.0	31.91	0.0	0.0	0.98	0.0

[a]Mean value of three samples at each time

Table 6 AUCs (μg/ml·min) of 17AAG in plasma and tissues of mice injected i.v. with a 60 mg/kg dose of microdispersed 17AAG

Plasma	Brain	Heart	Lung	Liver	Kidney	Spleen	Skeletal muscle
1,738	940	9,819	290,131	59,630	2,639	30,019	408

i.v., i.p., and oral studies with lyophilized 17AAG a dose of 40 mg/kg was used, a dose that did not result in any obvious drug-related toxicity during any of the three pharmacokinetic studies.

Plasma pharmacokinetics. Lyophilized 17AAG delivered i.v. at 40 mg/kg produced "peak" plasma concentrations of 20.2–38.4 μg/ml 5 min after injection (Fig. 3). As with the previous i.v. pharmacokinetic studies, which used microdispersed 17AAG, the concentration versus time data for the lyophilized formulation were best fitted by a two-compartment open linear model, but with the new 17AAG formulation, plasma concentrations of 17AAG had fallen to less than the lower limit of quantitation by 240 min after injection. Noncompartmental analysis of these data indicated a 17AAG AUC of 912 μg/ml·min, which was approximately 50% greater than the AUC of 625 μg/ml·min produced by a 40 mg/kg i.v. dose of the original 17AAG formulation. As with the initial formulation of 17AAG, i.v. delivery of lyophilized 17AAG resulted in substantial plasma concentrations of 17AG, but also resulted in easily detectable concentrations of an as-yet-unidentified metabolite with a retention time of 5 min on the HPLC chromatogram (Fig. 3). As with 17AAG, both 17AG and the 5-min metabolite could not be detected in plasma later than 240 min after injection of 17AAG.

Tissue distribution. As observed after i.v. delivery of a 60 mg/kg dose of microdispersed 17AAG, a 40 mg/kg i.v. dose of lyophilized 17AAG was widely distributed to various tissues (Tables 8 and 9). Again, the highest tissue concentrations of 17AAG were observed in lung with progressively lower concentrations measured in liver, kidney, heart, spleen, skeletal muscle, and brain. 17AAG concentrations declined in all tissues with time and by 4–8 h were less than the lower limit of quantitation of the

Table 7 Concentrations of 17AG in plasma (μg/ml) and tissues (μg/g) of mice injected i.v. with a 60 mg/kg dose of microdispersed 17AAG

Time (min)	Plasma	Brain	Heart	Lung	Liver	Kidney	Spleen	Skeletal muscle
5	1.73[a]	0.10	1.52	11.08	21.62	1.48	1.08	0.0
10	1.35	0.11	2.25	9.34	16.5	2.6	1.42	0.0
15	2.88	0.1	3.02	6.45	11.89	2.71	2.07	0.0
30	3.51	0.12	2.35	9.38	15.24	3.66	2.3	0.0
45	2.58	0.20	4.27	7.39	14.7	5.95	1.91	0.0
60	1.15	0.22	16.26	5.5	11.63	4.24	2.47	0.0
90	1.66	0.16	1.88	6.9	12.54	4.06	3.03	0.0
120	1.44	0.27	2.35	5.98	39.37	8.01	2.97	0.0
180	0.77	0.13	10.59	6.97	12.11	12.35	1.92	0.0
240	0.23	0.13	0.0	5.25	10.77	5.73	1.35	0.0
360	0.55	0.08	0.0	6.58	4.2	1.32	1.64	0.0
420	0.61	0.03	0.0	3.8	4.57	0.71	1.08	0.0
960	0.42	0.07	0.0	0.4	2.26	0.0	0.0	0.0
1440	0.28	0.18	0.0	0.0	0.83	0.0	0.0	0.0

[a]Mean value of three samples at each time

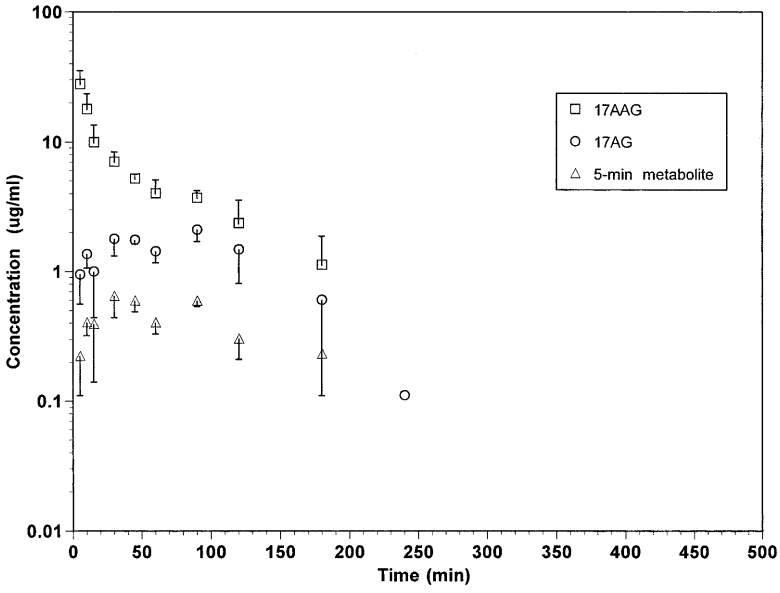

Fig. 3 Concentrations of 17AAG (□), 17AG (○), and 5-min metabolite (Δ) detected in plasma of female CD_2F_1 mice given a 40 mg/kg i.v. dose of lyophilized 17AAG. Symbols represent the means from three mice at each time-point, and error bars represent one SD

HPLC assay. All tissues examined also contained measurable concentrations of 17AG (Table 10). Tissue concentrations of 17AG increased during the first hour after injection of 17AAG and then progressively declined to undetectable concentrations by 6–8 h.

Bioavailability studies. Subsequent to the 40 mg/kg i.v. study, a study was performed wherein 17AAG was administered i.p. After i.p. delivery of a 40 mg/kg dose of 17AAG, plasma concentrations of 17AAG increased gradually with a peak concentration of approximately 11 μg/ml observed at 60 min, and then declined to less than the lower limit of quantitation by 240 min (Fig. 4). Plasma concentration versus time profiles of 17AG and the 5-min metabolite followed similar time courses. Modeled in a noncompartmental fashion, the 17AAG AUC produced by a 40 mg/kg i.p. dose was 900 μg/ml·min, indicating a bioavailability of approximately 99% (Table 2). In addition to modeling these plasma concentration versus time data in a noncompartmental fashion, compartmental modeling was also employed. The data were best fitted by a one-compartment open linear model with first-order absorption from the peritoneum, and resulted in values for V, k_a, and k_e of 1445 ml/kg, 0.03 min^{-1}, and 0.029 min^{-1}, respectively (Table 1).

A final pharmacokinetic study was undertaken wherein a 40 mg/kg dose of 17AAG was administered by gavage (Fig. 5). Peak plasma 17AAG concentrations of approximately 2.5 μg/ml were measured 15 min after administration of drug. As in previous studies with lyophilized 17AAG, 17AG and the metabolite with a retention time of 5 min were observed in plasma. Modeled in a noncompartmental fashion, the 17AAG AUC produced by a 40 mg/kg oral dose was 222 μg/ml·min, indicating a bioavailability of approximately 24% (Table 2). In addition to modeling these plasma concentration versus time data in a noncompartmental fashion, compart-

Table 9 AUCs (μg/ml·min) of 17AAG in plasma and tissues of mice injected i.v. with a 40 mg/kg dose of lyophilized 17AAG

Plasma	Brain	Heart	Lung	Liver	Kidney	Spleen	Skeletal muscle
912	161	1810	4309	6158	4167	2133	1105

Table 8 Concentrations of 17AAG in plasma (μg/ml) and tissues (μg/g) of mice injected i.v. with a 40 mg/kg dose of lyophilized 17AAG

Time (min)	Plasma	Brain	Heart	Lung	Liver	Kidney	Spleen	Skeletal muscle
5	27.56[a]	5.08	66.69	294.04	89.01	91.63	10.49	24.1
10	17.73	1.75	36.76	123.59	86.84	70.94	17.68	16.38
15	9.85	1.89	21.57	59.14	57.98	39.02	19.95	12.56
30	6.99	0.86	14.65	42.18	66.06	40.69	19.44	5.67
45	5.18	0.78	12.01	33.55	51.62	29.38	13.67	12.33
60	3.97	0.81	10.58	14.94	42.54	27.2	19.47	9.57
90	3.68	0.60	6.26	10.90	30.05	17.94	7.43	3.4
120	2.34	0.47	4.65	5.20	20.92	12.92	7.29	3.69
180	1.12	0.40	3.17	4.38	7.16	6.7	4.5	16.45
240	0.0	0.16	0.47	1.13	0.73	0.72	0.94	0.3
360	0.0	0.0	0.0	0.0	0.10	0.18	0.25	0.0

[a]Mean value of three samples at each time

Table 10 Concentrations of 17AG in plasma (μg/ml) and tissues (μg/g) of mice injected i.v. with a 40 mg/kg dose of lyophilized 17AAG

Time (min)	Plasma	Brain	Heart	Lung	Liver	Kidney	Spleen	Skeletal muscle
5	0.94[a]	0.12	1.94	8.16	15.33	3.65	1.29	0.84
10	1.35	0.13	2.35	5.36	21.61	6.18	2.92	0.93
15	0.99	0.21	2.76	3.53	17.46	5.09	2.36	0.90
30	1.77	0.15	2.86	4.94	23.33	9.87	4.46	0.84
45	1.74	0.19	3.94	4.94	23.09	9.52	5.28	2.11
60	1.42	0.21	3.38	4.73	20.48	9.27	5.30	1.70
90	2.09	0.21	3.2	4.26	20.88	8.40	4.52	0.90
120	1.47	0.22	2.81	3.21	18.97	7.64	4.48	1.13
180	0.60	0.09	2.9	2.92	10.18	5.27	3.04	0.49
240	0.11	0.09	0.84	1.79	5.59	2.90	2.54	0.41
360	0.0	0.07	0.12	0.93	2.43	0.97	1.12	0.28

[a]Mean value of three organs at each time

mental modeling was also employed. The data were best fitted by a two-compartment open linear model with first-order absorption, and resulted in values for V, k_a, k_{cp}, k_{pc}, and k_e of 3744 ml/kg, 0.041 min^{-1}, 0.045 min^{-1}, 0.0084 min^{-1}, and 0.056 min^{-1}, respectively (Table 1).

Discussion

Ideally, rational use of any drug should consider the pharmacology of that drug. This philosophy may receive even more emphasis in antineoplastic chemotherapy as increased effort is being devoted to developing target-directed agents [1, 2, 6, 7, 10, 16, 21, 27, 30, 31, 37]. In the specific case of 17AAG, a heat-shock protein-interactive drug that has recently entered clinical trials [3, 8, 12], a number of aspects of its pharmacology have been described [5, 9, 11, 15, 18, 20, 22, 24, 25, 26, 28, 32, 33, 34, 35, 38, 39, 40, 43, 44]. The proposed mechanism by which 17AAG downregulates certain oncoproteins, and thereby presumably reduces cell growth, has been investigated and described in detail [5, 9, 11, 18, 20, 22, 24, 25, 26, 28, 32, 33, 34, 35, 38, 39, 40, 43, 44]. Similarly, the enzymology involved in 17AAG metabolism and the structures of some of the resulting metabolites have been characterized [15]. The data presented here represent another part of the effort to produce preclinical pharmacology data that would enhance the design of clinical trials and development of 17AAG. In that regard, a number of aspects of the current studies warrant discussion.

The HPLC method used in this study to quantify 17AAG [15] should be applicable to clinical trials. Such measurements should facilitate integration of the pharmacokinetics of 17AAG with the clinical effects it produces. Obviously, the HPLC method should also be applicable to additional preclinical studies that might be undertaken in concert with, or subsequent to, the initiation of clinical trials of 17AAG.

The use of several doses, routes and formulations of 17AAG in the studies presented allowed several other relevant aspects of 17AAG pharmacology to be explored. Increasing doses of 17AAG produced increased plasma concentrations and exposures of 17AAG.

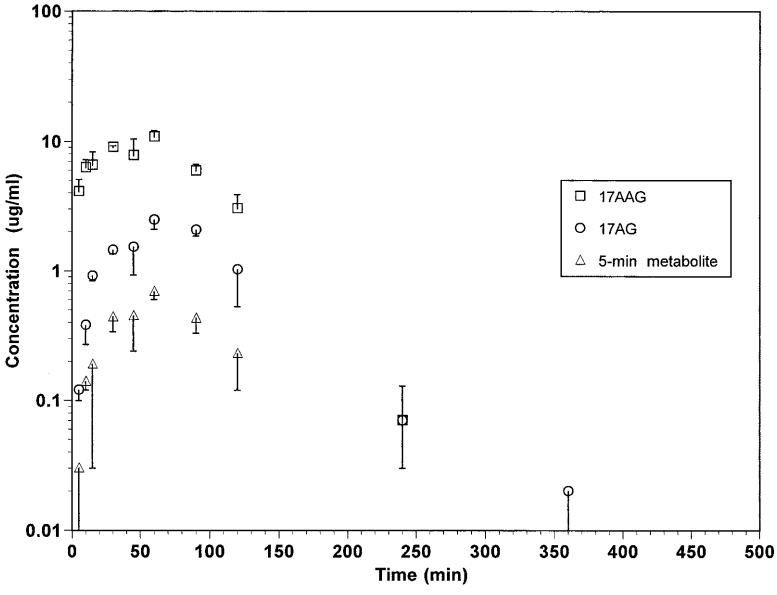

Fig. 4 Concentrations of 17AAG (□), 17AG (○), and 5-min metabolite (Δ) detected in plasma of female CD_2F_1 mice given a 40 mg/kg i.p. dose of lyophilized 17AAG. Symbols represent the means from three mice at each time-point, and error bars represent one SD

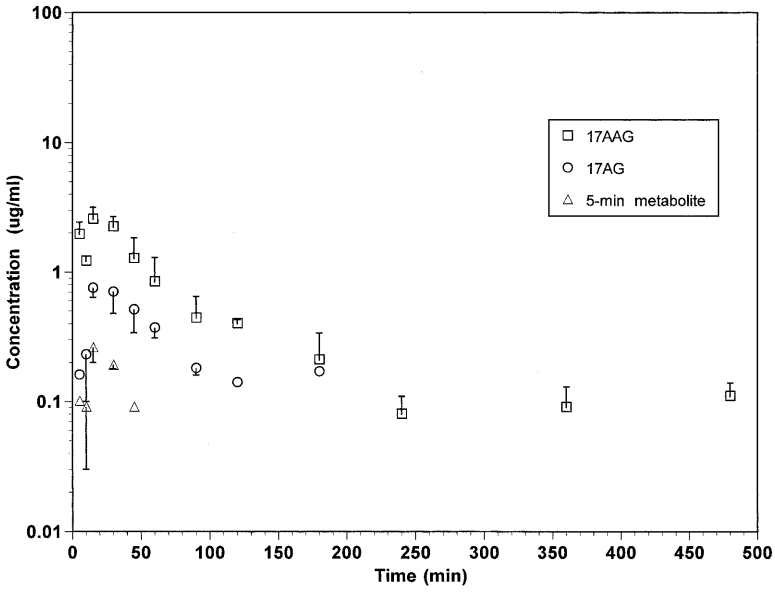

Fig. 5 Concentrations of 17AAG (□), 17AG (○), and 5-min metabolite (Δ) detected in plasma of female CD_2F_1 mice given a 40 mg/kg oral dose of lyophilized 17AAG. Symbols represent the means from three mice at each time-point, and error bars represent one SD

Whereas the increase in dose from 26.67 to 40 mg/kg was associated with a proportional increase in plasma AUC and no change in CL_{tb}, the increase in dose from 40 to 60 mg/kg produced a disproportionately large increase in the AUC, and a corresponding decrease in CL_{tb}. Whether this reflects saturation of a 17AAG clearance mechanism, such as its conversion to 17AG or its biliary excretion, is not known.

It is obvious that alteration of the formulation of 17AAG from a microdispersed to a lyophilized preparation was associated with rather profound changes in the behavior of 17AAG. A 60 mg/kg i.v. dose, which was without untoward effects when delivered as the microdispersed preparation, proved lethal to more than 50% of the first eight mice given the same dose as the lyophilized preparation. Although the exact cause for this difference is not known, it is striking that the 40 mg/kg dose of lyophilized 17AAG produced "peak" plasma concentrations of 17AAG that were approximately twice those produced by a 40 mg/kg i.v. dose of microdispersed 17AAG and even greater than the "peak" 17AAG concentrations measured in plasma of mice given 60 mg/kg of microdispersed drug. In addition to the higher "peak" plasma 17AAG concentrations produced by lyophilized 17AAG, the plasma AUC associated with the 40 mg/kg dose of i.v. lyophilized 17AAG was approximately 50% greater than the AUC associated with the same dose of the microdispersed preparation. Furthermore, while both microdispersed and lyophilized preparations of 17AAG were metabolized to 17AG, plasma and tissues of mice treated with lyophilized 17AAG contained an additional, as-yet-unidentified, 17AAG metabolite.

As with plasma pharmacokinetics, the two 17AAG formulations differed in their tissue distribution and exposure. Whereas 17AAG delivered as either formulation distributed widely to tissues, drug delivered as the microdispersed formulation was highly concentrated in the lung and liver and produced lower "peak" plasma concentrations than those produced by the lyophilized formulation. This is quite compatible with trapping of microparticulate material in the first capillary bed encountered after i.v. administration and subsequent trapping of circulating material by the hepatic and, to a lesser extent, splenic reticuloendothelial system. Furthermore, drug delivered as the microdispersed formulation persisted in most tissues for longer than did 17AAG delivered as the lyophilized formulation. Also, the microdispersed form of 17AAG resulted in strikingly larger AUCs in brain, heart, lungs, and liver than did the lyophilized form. These differences are still striking after one considers that tissue distribution and concentrations were determined in mice given 60 mg/kg of microdispersed 17AAG and 40 mg/kg of lyophilized 17AAG.

The results of studies wherein 17AAG was given by the i.p. and oral routes showed that the bioavailability by the former route was essentially 100% while that of the latter route was much less. The excellent bioavailability of 17AAG after i.p. delivery means that antitumor efficacy studies should be able to utilize that route instead of the logistically much more difficult i.v. route. The relatively low bioavailability of 17AAG after oral administration may not be surprising. 17AAG is a known substrate for cytochrome P450 3A4 and is likely a substrate for that isoform, and possibly p-glycoprotein, in the small intestine. This raises the possibility of modulating the oral bioavailability of 17AAG by combining it with drugs such as cyclosporine [23, 41, 42] or ketoconazole [14, 17, 19]. Successful studies in that regard would then facilitate evaluation of oral 17AAG, a route that might be the most desirable way to produce the prolonged 17AAG exposure that might be required for antitumor activity.

In summary, we characterized the plasma pharmacokinetics and tissue concentrations associated with a variety of doses and routes of administration of 17AAG.

These data have assisted in the design of clinical trials of 17AAG that have been recently initiated [3, 8, 12] and others that are being planned.

Acknowledgement We thank the University of Pittsburgh Cancer Institute for its confidence in our abilities.

References

1. Adams J, Palombella VJ, Sausville EA, Johnson J, Destree A, Lazarus DD, Maas J, Pien CS, Prakash S, Elliott PJ (1999) Proteasome inhibitors: a novel class of potent and effective antitumor agents. Cancer Res 59:2615
2. Adjei AA (2000) Signal transduction pathway targets for anticancer drug discovery. Curr Pharm Des 6:361
3. Agnew EB, Neckers LM, Hehman HE, Morrison G, Hamilton JM, Monahan BP, Grem JL, Takimoto CH (2000) Human plasma pharmacokinetics of the novel antitumor agent, 17-allylaminogeldanamycin (AAG) using a new HPLC-based analytic assay. Proc Am Assoc Cancer Res 41:701
4. Akaike H (1979) A Bayesian extension of the minimal AIC procedures of autoregressive model fitting. Biometrika 66:237
5. An WG, Schnur RC, Neckers L, Blagosklonny MV (1997) Depletion of $p185^{erbB2}$, and Raf-1 and mutant p53 proteins by geldanamycin derivatives correlates with antiproliferative activity. Cancer Chemother Pharmacol 40:60
6. Arbuck SG, Takimoto CH (1998) An overview of topoisomerase I-targeting agents. Semin Hematol 35[3 Suppl 4]:3
7. Autexier C (1999) Telomerase as a possible target for anticancer therapy. Chem Biol 6:R299
8. Banerji U, Walton MI, Orr R, Kelland L, Judson IR, Workman P (2000) Development and validation of pharmacodynamic end points in tumor and normal tissue to assess the effect of the HSP90 molecular chaperone inhibitor 17-allylamino-17-demethoxy geldanamycin (17-AAG). Proc Am Assoc Cancer Res 41:721
9. Blagosklonny MV, Toretsky J, Neckers L (1995) Geldanamycin selectively destabilizes and conformationally alters mutated p53. Oncogene 11:933
10. Buolamwini JK (2000) Cell cycle molecular targets in novel anticancer drug discovery. Curr Pharm Des 6:379
11. Chavany C, Mimnaugh E, Miller P, Bitton R, Nguyen P, Trepel J, Whitesell L, Schnur R, Moyers JD, Neckers L (1996) $p185^{erbB2}$ Binds to GRP94 in vivo. J Biol Chem 271:4974
12. Clarke PA, Hostein I, George M, Maillard K, Maloney A, Walton M, Swift I, Cunningham D, Wooster R, Workman P (2000) DNA array technology in the molecular pharmacology of colorectal cancer. Proc Am Assoc Cancer Res 41:721
13. D'Argenio DZ, Schumitzky A (1979) A program package for simulation and parameter estimation in pharmacokinetic systems. Comput Methods Programs Biomed 9:115
14. Dresser GK, Spence JD, Bailey DG (2000) Pharmacokinetic-pharmacodynamic consequences and clinical relevance of cytochrome P450 3A4 inhibition. Clin Pharmacokinet 38:41
15. Egorin MJ, Rosen DM, Wolff JH, Callery PS, Musser SM, Eiseman JL (1998) Metabolism of 17-(allylamino)-17-demethoxygeldanamycin (NSC 330507) by murine and human hepatic preparations. Cancer Res 58:2385
16. Gibbs JB (2000) Anticancer drug targets: growth factors and growth factor signaling. J Clin Invest 105:9
17. Gomez DY, Wacher VJ, Tomlanovich SJ, Herbert MF, Benet LZ (1995) The effects of ketoconazole on the intestinal metabolism and bioavailability of cyclosporine. Clin Pharmacol Ther 58:15
18. Hartman F, Horak EM, Cho C, Luupu R, Bolen JB, Stetler SM, Pfreundschuh M, Waldmann TA, Horak ID (1997) Effects of the tyrosine-kinase inhibitor geldanamycin on ligand-induced Her-2/neu activation, receptor expression and proliferation of Her-2-positive malignant cell lines. Int J Cancer 70:221
19. Jordan WC (1998) The effectiveness of combined saquinavir and ketoconazole treatment in reducing HIV viral load. J Natl Med Assoc 90:622
20. Kelland LR, Sharp SY, Rogers PM, Myers TG, Workman P (1999) DT-diaphorase expression and tumor cell sensitivity to 17-allylamino,17-demethoxygeldanamycin, an inhibitor of heat shock protein 90. J Natl Cancer Inst 91:1940
21. Keshet E, Ben-Sasson SA (1999) Anticancer drug targets: approaching angiogenesis. J Clin Invest 104:1497
22. McIlwrath AJ, Brunton VG, Brown R (1996) Cell-cycle arrests and p53 accumulation induced by geldanamycin in human ovarian tumour cells. Cancer Chemother Pharmacol 37:423
23. Meerum Terwogt JM, Malingre MM, Beijnen JH, ten Bokkel Huinink WW, Rosing H, Koopman J, van Tellingen O, Swart M, Schellens JHM (1999) Coadministration of oral cyclosporin A enables oral therapy with paclitaxel. Clin Cancer Res 5:3379
24. Miller P, DiOrio C, Moyer M, Schnur RC, Bruskin A, Cullen W, Moyer JD (1994) Depletion of the erbB-2 gene product p185 by benzoquinoid ansamycins. Cancer Res 54:2724
25. Miller P, Schnur RC, Barbacci E, Moyer MP, Moyer JD (1994) Binding of benzoquinoid ansamycins to p100 correlates with their ability to deplete the *erb*B2 gene product p185. Biochem Biophys Res Commun 201:1313
26. Mimnaugh E, Chavany C, Neckers LM (1996) Polyubiquitination and proteasomal degradation of the p185c-erbB2 receptor protein-tyrosine kinase induced by geldanamycin. J Biol Chem 271:22796
27. Monks A, Scudiero DA, Johnson GS, Paull KD, Sausville EA (1997) The NCI anti-cancer drug screen: a smart screen to identify effectors of novel targets. Anticancer Drug Des 12:533
28. Neckers L, Schulte TW, Mimnaugh E (1999) Geldanamycin as a potent anti-cancer agent: its molecular target and biochemical activity. Invest New Drugs 17:361
29. Rocci ML, Jusko WJ (1983) LAGRAN program for area and moments in pharmacokinetic analysis. Comput Programs Biomed 16:203
30. Sausville EA, Feigal E (1999) Evolving approaches to cancer drug discovery and development at the National Cancer Institute, USA. Ann Oncol 10:1287
31. Sausville EA, Zaharevitz D, Gussio R, Meijer L, Louarn-Leost M, Kun Schultz R, Lahusen T, Headlee D, Stinson S, Arbuck SG, Senderowicz AM (1999) Cyclin-dependent kinases: initial approaches to exploit a novel therapeutic target. Pharmacol Ther 82:285
32. Schneider C, Sepp-Lorinzino L, Nimmersgen E, Ouerfelli O, Danishefsky S, Rosen N, Hartl FU (1996) Pharmacologic shifting of a balance between protein refolding and degradation mediated by Hsp90. Proc Natl Acad Sci USA 93:14536
33. Schnur RC, Corman ML, Gallaschun RJ, Cooper BA, Dee MF, Doty JL, Muzzi ML, DiOrio CI, Barbacci EG, Miller PE, Pollack VA, Savage DM, Sloan DE, Pustilnik LR, Moyer JD, Moyer MP (1995) erbB-2 Oncogene inhibition by geldanamycin derivatives: synthesis, mechanism of action, and structure-activity relationships. J Med Chem 38:3813
34. Schnur RC, Corman ML, Gallaschun RJ, Cooper BA, Dee MF, Doty JL, Muzzi ML, Moyer JD, DiOrio CI, Barbacci EG, Miller PE, O'Brien AT, Morin MJ, Foster BA, Pollack VA, Savage DM, Sloan DE, Pustilnik LR, Moyer MP (1995) Inhibition of the oncogene product $p185^{erbB-2}$ in vitro and in vivo by geldanamycin and dihydrogeldanamycin derivatives. J Med Chem 38:3806
35. Schulte TW, Blagosklonny MV, Ingui C, Neckers L (1995) Disruption of the Raf-1-Hsp90 molecular complex results in destabilization of Raf-1 and loss of Raf-1-Ras association. J Biol Chem 270:24585
36. Shah VP, Midha KK, Dighe S, McGilvery IJ, Skelly JP, Yacobi A, Layloff T, Viswanathan CE, Cook CE, McDowall RD, Pittman KA, Spector S (1991) Analytical methods validation: bioavailability, bioequivalence and pharmacokinetic studies. Eur J Drug Metab Pharmacokinet 16:249
37. Shapiro GI, Harper JW (1999) Anticancer drug targets: cell cycle and checkpoint control. J Clin Invest 104:1645

38. Stebbins CE, Russo AA, Schneider C, Rosen N, Hartl FU, Pavletich NP (1997) Crystal structure of and Hsp90-geldanamycin complex: targeting of a protein chaperone by an antitumor agent. Cell 89:239
39. Supko JG, Hickman RL, Grever M, Malspeis L (1995) Preclinical pharmacological evaluation of geldanamycin as an antitumor agent. Cancer Chemother Pharmacol 36:305
40. Uehara Y, Hori M, Takeuchi T, Umezawa H (1986) Phenotypic change from transformed to normal induced by benzoquinoid ansamycins accompanies inactivation of p60src in rat kidney cells infected with Rous sarcoma virus. Mol Cell Biol 6:2198
41. Van Asperen J, van Tellingen O, Sparreboom A, Schinkel AH, Borst P, Nooijen WJ, Beijnen JH (1997) Enhanced oral bioavailability of paclitaxel in mice treated with the P-glycoprotein blocker SDZ PSC 833. Br J Cancer 76:1181
42. Van Asperen J, van Tellingen O, van der Valk MA, Rozenhart M, Beijnen JH (1998) Enhanced oral absorption and decreased elimination of paclitaxel in mice cotreated with cyclosporin A. Clin Cancer Res 4:2293
43. Whitesell L, Cook P (1996) Stable and specific binding of heat shock protein 90 by geldanamycin disrupts glucocorticoid receptor function in intact cells. Mol Endocrinol 10:705
44. Whitesell L, Mimnaugh EG, De Costa B, Myers CE, Neckers LM (1994) Inhibition of heat shock protein HSP90-pp60$^{v\text{-}src}$ heteroprotein complex formation by benzoquinone ansamycins: essential role for stress proteins in oncogenic transformation. Proc Natl Acad Sci U S A 91:8324
45. Yeh KC, Kwan KC (1978) A comparison of numerical integrating algorithms by trapezoidal, LaGrange and spline approximation. J Pharmacokinet Biopharm 6:79